JOURNAL OF GEOPHYSICAL RESEARCH: OCEANS, VOL. 118, 1239–1256, doi:10.1002/jgrc.20138, 2013

Physical controls on hypoxia in Chesapeake Bay: A numerical modeling study

Malcolm E. Scully[1]

Received 25 November 2012; revised 18 February 2013; accepted 19 February 2013; published 14 March 2013.

[1] A three-dimensional circulation model with a relatively simple dissolved oxygen model is used to examine the role that physical forcing has on controlling hypoxia and anoxia in Chesapeake Bay. The model assumes that the biological utilization of dissolved oxygen is constant in both time and space, isolating the role that physical forces play in modulating oxygen dynamics. Despite the simplicity of the model, it demonstrates skill in reproducing the observed variability of dissolved oxygen in the bay, highlighting the important role that variations in physical forcing have on the seasonal cycle of hypoxia. Model runs demonstrate significant changes in the annual integrated hypoxic volume as a function of river discharge, water temperature, and wind speed and direction. Variations in wind speed and direction had the greatest impact on the observed seasonal cycle of hypoxia and large impacts on the annually integrated hypoxic volume. The seasonal cycle of hypoxia was relatively insensitive to synoptic variability in river discharge, but integrated hypoxic volumes were sensitive to the overall magnitude of river discharge at annual time scales. Increases in river discharge were shown to increase hypoxic volumes, independent from the associated biological response to higher nutrient delivery. However, increases in hypoxic volume were limited at very high river discharge because increased advective fluxes limited the overall length of the hypoxic region. Changes in water temperature and its control on dissolved oxygen saturation were important to both the seasonal cycle of hypoxia and the overall magnitude of hypoxia in a given year.

Citation: Scully, M. E. (2013), Physical controls on hypoxia in Chesapeake Bay: A numerical modeling study, *J. Geophys. Res. Oceans*, *118*, 1239–1256, doi:10.1002/jgrc.20138.

1. Introduction

[2] Every summer, the sub-pycnocline waters in the central portion of Chesapeake Bay experience low dissolved oxygen (hypoxia) or the complete lack of dissolved oxygen (anoxia) for extended periods of time. Direct observations of hypoxic and anoxic bottom waters in Chesapeake Bay were first made during the 1930s [*Newcombe and Horne*, 1938]. Since the early 1950s, continued water quality sampling demonstrates that the depletion of dissolved oxygen in bottom waters is a persistent seasonal phenomenon in the bay [e.g., *Hagy et al*. 2004; *Kemp et al*., 2005; *Murphy et al*., 2011]. Typically, dissolved oxygen levels decrease during the spring, with the onset of anoxic/hypoxic conditions occurring in sub-pycnocline waters of the deeper portions ($h > 15$ m) of the bay in mid to late May. A significant volume of water below the pycnocline generally remains devoid of oxygen until mid to late September. While the seasonal cycle of hypoxia in the bay is a robust and repeatable phenomenon, the spatial extent and duration vary considerably from year to year [*Hagy et al*. 2004]. Work carried out in the 1980s suggested that both the persistence and duration of hypoxic conditions had increased since the first measurements made in the 1930s [*Officer et al*., 1984]. This trend has continued, and there is considerable evidence suggesting that hypoxic volumes increased in the early 1980s and remains above pre-1980s levels today [*Hagy et al*., 2004; *Kemp et al*., 2005]. A number of these studies have suggested that the increased hypoxic volumes are largely the result of anthropogenic alteration of the ecosystem, with the most common explanation being eutrophication resulting from increased nutrient loads to the systems.

[3] Although it is generally accepted that the increased nutrient loads that are delivered to the system have increased the extent and severity of low oxygen conditions, studies that directly correlated nutrient loads to interannual variations in hypoxic volume often fail to explain the majority of the variability [*Hagy et al*., 2004; *Scully*, 2010a; *Murphy et al*., 2011]. These studies explain a significantly larger fraction of the interannual variability when they include both nutrient loading and the variability in physical forcing. River discharge, wind forcing, water temperature, and vertical density stratification all play a role in modulating dissolved oxygen in Chesapeake. These physical forces all exhibit significant interannual variability, making it difficult to clearly isolate the role of nutrient loading. Understanding

[1]Applied Ocean Physics and Engineering, Woods Hole Oceanographic Institution, Woods Hole, MA, USA.

Corresponding author: M. E. Scully, Woods Hole Oceanographic Institution, Mail Stop 10, Woods Hole, MA 02543, USA. (mscully@whoi.edu)

2169-9275/13/10.1002/jgrc.20138

the role of physical forcing is of far greater significance than purely academic interest. Billions of dollars have been spent to reduce nutrient inputs into the bay, with the explicit goal of reducing the duration and severity of hypoxia [*Butt and Brown*, 2000]. In order to understand the effectiveness of these efforts, it is essential to quantify the importance of physical processes in modulating hypoxic volumes in Chesapeake Bay. This paper attempts to quantify the role that physical forcing plays in modulating dissolved oxygen by using a numerical circulation model with a highly simplified model for oxygen dynamics. The seasonal and interannual variability in dominant physical processes that are expected to impact dissolved oxygen are presented in section 2. The model used in this study is described in section 3. Results from the model are given in section 4 and discussed in section 5. Summary and conclusions are given in section 6.

2. Physical Forcing

[4] Before presenting the model, it is instructive to review the dominant physical forces and how they are expected to influence dissolved oxygen dynamics in Chesapeake Bay, and to briefly quantify their variability. To do this, we use the U.S. Geological Survey (USGS) gauging station at Conowingo, MD to estimate river discharge from the Susquehanna River (daily values, 1967–2010), the Chesapeake Bay Program (CBP) Water Quality Database to quantify vertical salinity stratification (monthly to bimonthly cruises, 1990–2006), and the Thomas Point Light (TPL) Buoy to examine wind speed and direction and water temperature (hourly data, 1986–2011). Figure 1 shows the location of several CBP stations and TPL.

2.1. River Discharge

[5] There are numerous small rivers and creeks that enter Chesapeake Bay, but the majority of the river discharge (>90%) enters through the Susquehanna, Potomac, and James Rivers. The Susquehanna River delivers over 60% of the riverine-derived freshwater to the system with a strong seasonal hydrograph. Peak discharge typically occurs in early April before decreasing throughout the summer months (Figure 2a). The vertical salinity stratification lags the river discharge with maximum values of stratification typically observed in May (Figure 2b). It is commonly assumed that both the timing and strength of river discharge plays a fundamental role in controlling both the seasonal cycle of hypoxia and its interannual variability [*Taft et al.*, 1980; *Officer et al.*, 1984; *Kemp et al.*, 2005]. Conventional wisdom assumes that the strength of the vertical density gradient directly controls the vertical flux of oxygen through the pycnocline. Thus, it is assumed that the high river discharge during the spring months leads to increased density stratification during the summer and that this increased stratification during the summer fundamentally controls the supply of dissolved oxygen to sub-pycnocline waters. It follows that extensive hypoxia occurs in years with higher than average spring river discharge because of the river-discharge dependence of vertical density stratification. Thus, the magnitude of river discharge is thought to be one of the most important physical variables in controlling interannual variations in hypoxia in Chesapeake Bay, independent of the nutrient loads that the river discharge delivers to the system.

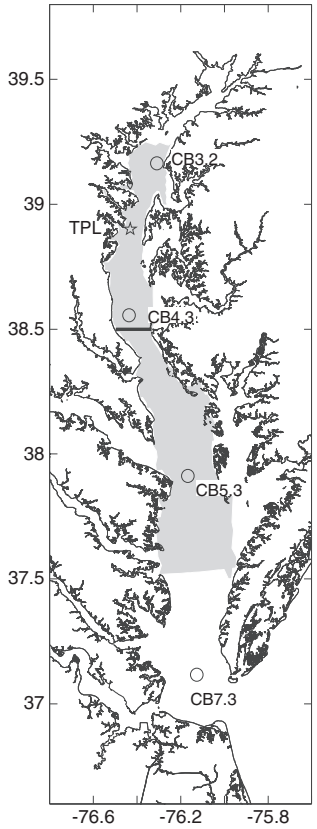

Figure 1. Map of Chesapeake Bay showing the location of select Chesapeake Bay Program Water Quality Stations (circles) and the Thomas Point Light Tower (star). The shaded region indicates the region used for the analysis, with the solid black line separating the "upper" bay from the "lower" bay.

2.2. Water Temperature

[6] Water temperature in Chesapeake Bay exhibits both strong seasonal and interannual variability (Figure 2c). At both seasonal and annual time scales, the observed water temperature at TPL is strongly correlated with the observed air temperature (data not shown). Seasonally, water temperature peaks in early August and reaches its minimum in late January. In addition to the seasonal cycle, there is considerable interannual variability. The difference between the maximum and minimum monthly averaged temperatures observed at TPL (1986–2011) varied from roughly 3 to 7°C depending on the month, with greater variability during the winter. Annually averaged temperatures can vary by more than 3°C. With the relatively strong vertical salinity differences that occur in the bay, temperature only plays a minor role in controlling stratification. Even when thermal stratification peaks in June, it still represents less than 15% of the top-to-bottom density difference in the main stem of Chesapeake Bay (data not shown). More important from a physical perspective is the role that temperature plays in controlling dissolved oxygen saturation. With the strong seasonal variation in temperature, dissolved oxygen saturation values in the bay peak at roughly 11.5 mg/L in February and reach a minimum of roughly 7.5 mg/L in August. At both the seasonal and interannual time scales, the lower saturation values associated with warmer waters could allow the drawdown to hypoxic/anoxic conditions to occur faster.

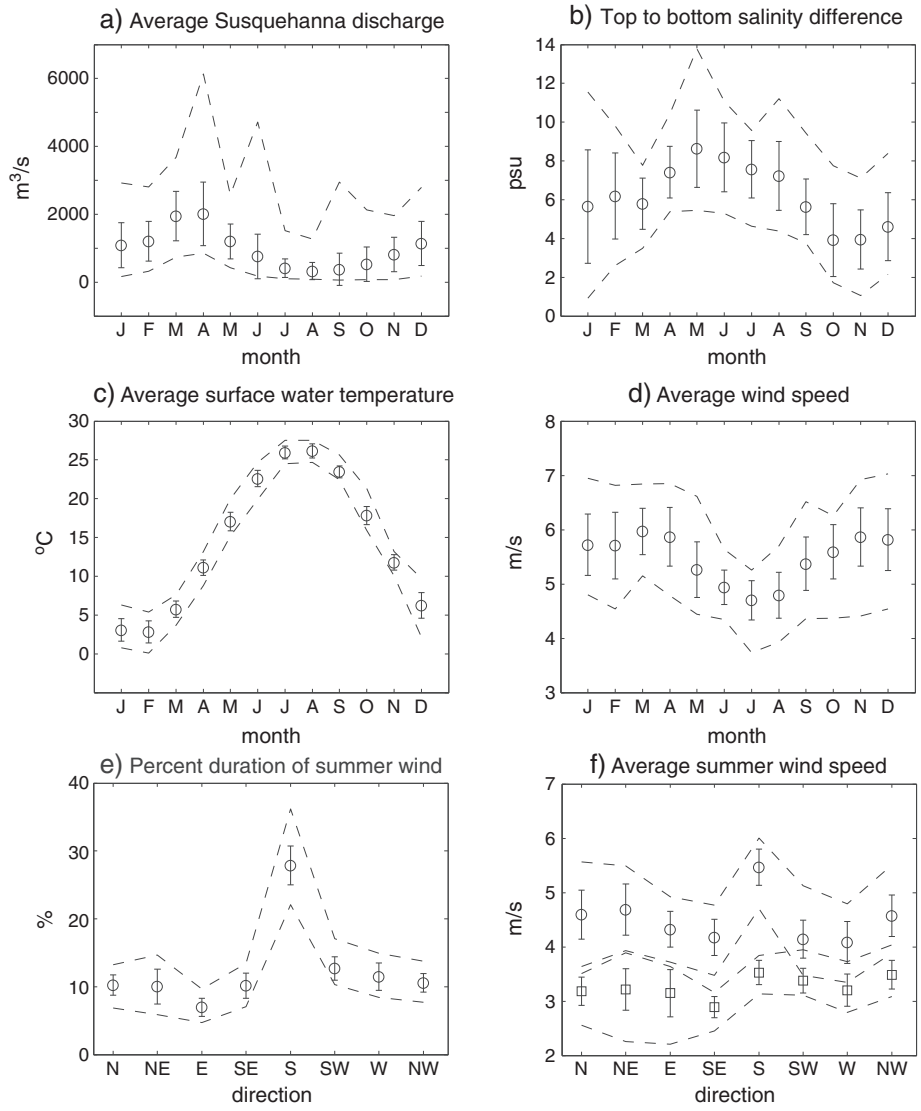

Figure 2. (a) Monthly averaged river discharge for Susquehanna River from USGS gauge at Conowingo, MD (1967–2010); (b) monthly averaged top-to-bottom salinity difference averaged over all main stem stations from the Chesapeake Bay Program water quality data base (1990–2006); (c) monthly averaged surface water temperature observed at National Data Buoy Center (NDBC) Thomas Point Light Station (TPL) (1986–2011); (d) monthly averaged wind speed observed at TPL (1986–2011); (e) percentage of time during summer months (May–August) that wind blows from eight equally spaced compass directions at TPL (1986–2011); (f) summer (May–August) wind speed averaged as a function of direction at TPL (1986–2011) (circles) and the NARR model data for the nearest location over the same time period (squares). In all plots, the vertical bars represent one standard deviation of the monthly averaged values, and the dashed horizontal lines represent the maximum and minimum monthly values observed.

2.3. Wind Speed and Direction

[7] As with river discharge and water temperature, wind forcing over Chesapeake Bay varies considerably at both seasonal and interannual time scales. Wind magnitude typically peaks in March and decreases throughout the spring and summer (Figure 2d). The lowest monthly averaged wind speeds occur in July and August with winds increasing during the fall and into the winter months. As with magnitude, wind direction also exhibits strong seasonal variability with winds from the north/northwest having the greatest occurrence during the winter, early spring, and late fall. During the late spring and summer months, winds shift to blow more from the south as the Bermuda-Azores High Pressure system becomes established. At TPL, during the summer (May–August), winds are observed from all directions, but winds from the south are most common (Figure 2e). Not only are winds from the south the most frequent during the summer months, but they also have the greatest averaged magnitude (Figure 2f). Winds from the west have the lowest observed average summer wind speeds at TPL. It is important to note that TPL is located in Chesapeake Bay (−76.421°W, 38.898°N) and measures wind speeds over water, which are generally higher than adjacent measurements made over land. Most regional atmospheric

models do not have sufficient resolution to capture these spatial gradients. For comparison, Figure 2f also shows the 10 m mean summer winds from the North American Regional Reanalysis (NARR) model for the station (−76.437°W, 39.036°N) closest to TPL. In Figure 2f, the winds at TPL have been adjusted to a height of 10 m assuming neutral stability following *Large and Pond* [1981]. The NARR summer winds are roughly 30% weaker than those observed at TPL and do not exhibit the strong directional asymmetry in wind speed. For example, measured winds from the west are more than 25% weaker than winds from the south at TPL, while the difference in the modeled NARR winds is less the 10%.

[8] These differences between the observed and modeled winds become important because both wind speed and direction can play an important role in modulating dissolved oxygen in the bay. At seasonal time scales, it is typically assumed that the decrease in wind mixing during the early summer reduces the supply of oxygen to subpycnocline waters via turbulent mixing, setting up hypoxic/anoxic conditions during the summer months. The increase in wind mixing from storms in the early fall is thought to play a key role in breaking down the stratification and ventilating bottom waters [*Goodrich et al*., 1987; *Blumberg and Goodrich*, 1990]. Thus, the seasonal variations in wind speed are thought to play an important role in controlling the seasonal cycle of hypoxia. In addition to driving direct vertical mixing, it has been suggested that wind-driven circulation interacts with the along-channel density field to modulate vertical density stratification [*Scully et al*., 2005; *Chen and Sanford*, 2009]. This process, known as wind straining, has been suggested to play an important role in modulating dissolved oxygen in western Long Island Sound [*Wilson et al*., 2008; *O'Donnell et al*., 2008]. *Wilson et al*. [2008] suggest that winds from the west in Long Island Sound increase stratification favoring more severe hypoxia. In the upper and middle reaches of Chesapeake Bay, down-estuary winds have been shown to enhance the residual circulation [*Wang*, 1979] and increase the vertical density stratification [*North et al*., 2004] consistent with axial wind straining. A more recent study by *Li and Li* [2011] suggests that lateral straining may partially offset longitudinal straining in modulating stratification.

[9] The enhanced residual circulation in response to down-estuary winds not only modulates stratification and hence vertical mixing, but it also can transport dissolved oxygen. Thus, along-channel wind forcing may provide an advective source of oxygen, particularly in the lower regions of the bay. In addition to driving along-estuary circulation, along-estuary winds also drive a strong rotational response in Chesapeake Bay. Strong lateral upwelling/downwelling of the pycnocline was documented by *Sanford et al*. [1990], and *Malone et al*. [1986] suggested that the lateral estuarine response to along-channel wind forcing may play an important role in driving exchange between surface and bottom waters. *Li and Li* [2012] use vorticity dynamics to explain why up-estuary winds demonstrate a stronger lateral response than down-estuary winds. This asymmetry in lateral response is important because *Scully* [2010b] demonstrated that the rotational response to along-channel wind forcing was a dominant mechanism for supplying oxygen to subpycnocline waters in the central region of Chesapeake Bay. At longer time scales, subtle shifts in wind direction related to climatological variability, were shown to be significantly correlated with interannual variations in hypoxic volume [*Scully* 2010a].

3. Model Description

[10] At both seasonal and interannual time scale, there is significant covariance in the physical processes that modulate dissolved oxygen in Chesapeake Bay. The transition from spring into summer is accompanied by increased density stratification, warmer waters, and the associated lower oxygen saturation and decreased wind mixing—all of which are thought to favor the development of summer hypoxia. The matter is further complicated by the seasonal and interannual variations in biological processes that also covary with the physical forcing. The inputs of nutrients are tightly coupled to freshwater inputs, respiration rates of organic matter are thought to be temperature dependent [*Smith and Kemp*, 1995], wind-driven circulation and mixing provide nutrients to surface waters fueling phytoplankton growth [*Malone et al*., 1986], and sediment resuspension and transport alter light availability, impacting phytoplankton dynamics and oxygen production. These highly complex interactions between the physical and biogeochemical processes that modulate dissolved oxygen make isolating the dependencies using sparse field data extremely challenging. Even in coupled hydrodynamic and biogeochemical models, these interactions can be so complex that quantifying the importance of specific physical forcing can be difficult.

[11] To address these complexities, we employ a three-dimensional circulation model coupled with the simplest possible model for oxygen dynamics. The goal is to isolate the role that variations in physical forces have on oxygen dynamics by assuming that biological processes are constant in both time and space. The model used in this study is based on the hydrodynamic component of the Chesapeake Bay ROMS Community Model (ChesROMS). A detailed description of ChesROMS is given in *Xu et al*. [2012]. The model utilizes a 150 by 100 curvilinear grid with 20 vertical terrain-following coordinates. In order to avoid pressure gradient errors associated with steeply sloping bathymetry, the original ChesROMS grid was slightly smoothed so that the slope parameter (r_0) is less than 0.4 (where $r_0 = \Delta h/h$, and h is water depth) [*Beckmann and Haidvogel*, 1993]. In smoothing the bathymetry, the maximum value of the channel thalweg was not changed.

[12] The model domain includes the nine largest tributaries to the bay, as well as the shelf region immediately adjacent to the bay mouth. River discharge forcing is based on the USGS gauging station daily mean values for each tributary. Water level forcing at the oceanic boundary includes nine tidal harmonic constituents and the observed nontidal water level based on an interpolation between observed values at Duck, NC and Wachepreque, VA. Surface boundary forcing, including short-wave solar radiation, long-wave radiation, and surface air humidity, pressure and temperature, was obtained from the NARR model. Wind forcing was based on the observed hourly winds at TPL and was assumed to be spatially uniform over the grid. The spatially varying NARR model winds were not used because they significantly underestimate the observed winds over water and do not capture the observed directional asymmetries (e.g., Figure 2f). The importance of spatial variations in wind forcing on Chesapeake Bay is the topic of ongoing research and is beyond the scope of this paper, and comparisons between spatially uniform observed winds and spatially varying NARR winds will be presented in another manuscript. The oceanic boundary is

forced with the temperature and salinity values from the World Ocean Atlas 2001. Turbulence closure is achieved using the k-ω model with the stability functions of *Kantha and Clayson* [1994], and the background diffusivity for both momentum and scalars is set to 1×10^{-5} m^2/s, consistent with previous modeling studies in Chesapeake Bay [*Li et al*., 2005; *Li and Li*, 2011]. No horizontal diffusivity was prescribed. While previous studies employing ChesROMS [e.g., *Scully*, 2010b] used a third-order upstream advection scheme for tracers, here we use the MPDATA advection scheme [*Smolarkiewicz and Margolin*, 1998]. The importance of background diffusivity, advections scheme, and the role of numerical mixing will be presented in a companion manuscript that is currently in preparation.

[13] To simulate oxygen dynamics in the simplest possible manner, we follow the methods of *Scully* [2010b] and introduce dissolved oxygen as an additional passive tracer in the model. Inside the estuarine portion of the domain, a spatially and temporally constant oxygen consumption of 1.7×10^{-4} mmol O_2/m^3/s (0.47 g O_2/m^3/day) is prescribed. Dissolved oxygen is introduced into the model via a surface flux. The surface flux of oxygen (F_{O2}) is prescribed as follows:

$$F_{o_2} = \left[O_2^{\text{sat}} - O_2\right] \tag{1}$$

where O_2 and O_2^{sat} are the surface oxygen concentration and concentration at saturation, respectively, and k (in cm/hr) is a wind speed (W) dependent piston velocity base on *Marino and Howarth* [1993], given as follows:

$$k = 2.97e^{0249W} \tag{2}$$

[14] Dissolved oxygen concentrations at both the oceanic and river boundaries were fixed to saturation values. Oxygen concentrations were not allowed to become negative, essentially imposing a respiration rate of 0 for anoxic conditions. While this ignores the potential influence of sulfide reduction, it is in keeping with the goal of using the simplest possible model for oxygen dynamics.

[15] In this paper, we focus our analysis on the 2004 calendar year. In order to obtain yearlong simulations for 2004, the model was initiated on 1 January 2003, using an idealized linearly varying temperature and salinity distribution, with no vertical density stratification. Initial oxygen concentrations were set to saturation.

[16] Using the 2004 simulation as the base model run, a series of sensitivity studies were conducted to examine the importance of changes in physical forcing, including river discharge, temperature, and wind speed and direction. These sensitivity runs are summarized in Table 1 and are briefly detailed in section 4.

Table 1. Table Outlining All Model Runs Conducted in This Study with a Brief Description of the Forcing and the Symbol Used in the Text

Model Symbol	Model Description
Base model run	
B	Base model run with realistic forcing
River discharge runs	
Qconst	River discharge in all tributaries set to annual average value
Q0.2	River discharge values reduced to 20% of observed values
Q0.5	River discharge values reduced to 50% of observed values
Q2	River discharge values increased by a factor of 2
Temperature runs	
Tsat5	Dissolved oxygen saturation assumed to be set by water with temperature of 5°C
Tsat25	Dissolved oxygen saturation assumed to be set by water with temperature of 25°C
T + 1	Air temperature was increased by 1 standard deviation based on monthly values
T − 1	Air temperature was decreased by 1 standard deviation based on monthly values
Wind Runs	
W-Jan	Winds from January were repeated for every month of yearlong simulation
W-July	Winds from July were repeated for every month of yearlong simulation
W + 0.10	Summer (May–August) wind magnitude was increased by 10%
W − 0.10	Summer (May–August) wind magnitude was decreased by 10%
W + 180°	Summer (May–August) wind direction was rotated 180°
W + 90°	Summer (May–August) wind direction was rotated positive 90°

4. Results

4.1. Base Model Run

[17] The main goal of this paper is not to conduct a comprehensive skill assessment of the model's ability to predict dissolved oxygen in Chesapeake Bay. A detailed evaluation of model skill will be presented in Friedrichs et al. (manuscript in preparation). Similarly, a comprehensive skill assessment of the model's ability to simulate hydrodynamic conditions (water elevation, temperature, salinity, and stratification) has been performed by *Xu et al*. [2012]. However, before proceeding with the detailed evaluation of the importance of physical processes, it is important to demonstrate that the model can reasonably predict the seasonal cycle of hypoxia that is observed in Chesapeake Bay. To that end, Figure 3 shows a comparison between the observed bottom dissolved oxygen concentration at four stations (CB3.2, CB4.3, CB5.3, CB7.2) from the Chesapeake Bay Program (CBP) and the corresponding model locations for the simulations for 2003–2005 (see Figure 1 for station locations). All four stations are located in the deep portion of the main channel, ranging from the upper bay (CB3.2) to lower bay (CB7.2). Despite the simplicity of the oxygen model, the seasonal cycle of hypoxia is simulated with reasonable skill. In addition to capturing the seasonal drawdown of oxygen in the spring and the subsequent ventilation in the fall, the model also captures some of the shorter time scale variability associated with strong wind/storm events (e.g., rapid rise in oxygen concentration at CB3.2 in late summer of 2003). While the model does reasonably well in simulating the summer hypoxic conditions, bottom oxygen concentrations are underpredicted during the winter months in the mid to lower regions of the bay. Presumably, respiration rates are considerably lower during this time of the year, and the assumption of constant respiration rates results in lower than observed oxygen concentrations. Similarly, observations of surface oxygen concentration are generally above saturation due to biological oxygen production. Clearly this simplified model cannot capture these supersaturated oxygen concentrations without including biological processes. However, even a model with

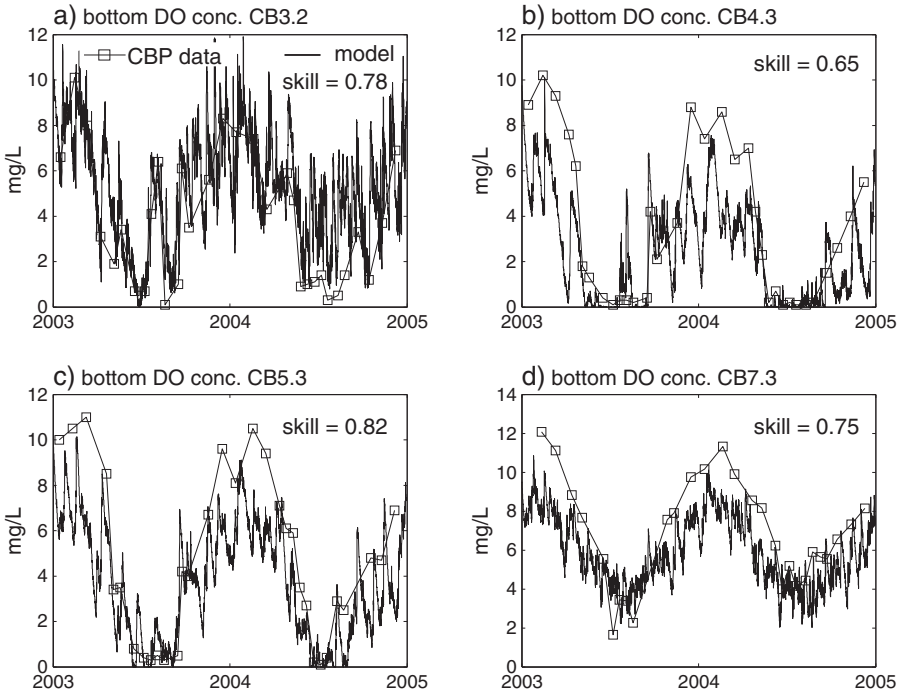

Figure 3. Comparison of bottom dissolved oxygen concentration from the model (solid line) with observations (squares) at selected stations from Chesapeake Bay Program (CBP) Water Quality Monitoring data. Locations span the upper bay (CB3.2) to lower bay (CB7.3) (see Figure 1 for locations). Model skill for each location was calculated following *Wilmott* [1981] based on a 2 day average of model output centered on the reported CBP sampling date.

no biological variability clearly predicts a seasonal cycle of hypoxia in the bay, clearly illustrating the importance of physical forcing.

[18] Changes in the total extent of hypoxic water in the bay can be quantified by calculating the total volume of water that has dissolved oxygen concentrations below a threshold value. Previous authors [e.g., *Hagy et al*., 2004; *Murphy et al*., 2011] have reported hypoxic volume based on dissolved oxygen concentrations of 2.0, 1.0, and 0.2 mg/L. We will refer to these thresholds as mildly hypoxic, strongly hypoxic, and anoxic in the remainder of the paper. Figure 4 shows a comparison between the modeled strongly hypoxic volume and volumes estimated by *Murphy et al*. [2011] from the CBP water quality data for the period 2003–2004. Even though the analysis in this paper focuses on 2004 and 2003 was only used for model initiation, we include the hypoxic volume calculations for 2003 in Figure 4 to highlight the ability of the model to capture the bulk variability in hypoxic volume in two different years. Not only does this relatively simple model capture both the onset and termination of hypoxic conditions in the bay, it also reasonably captures the total volumetric extent of summer hypoxia and some of the temporal variability.

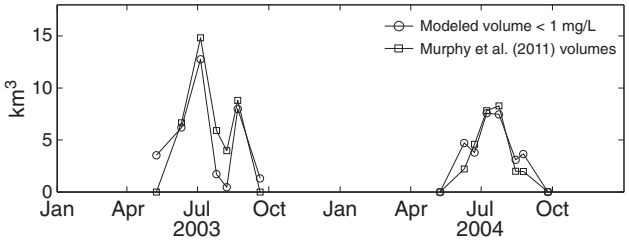

Figure 4. Comparison between modeled values (circles) of hypoxic volume (<1 mg/L) and the interpolated volumes of *Murphy et al*. [2011] (squares). The Murphy et al. data are based on the Chesapeake Bay Program (CBP) Water Quality Monitoring Program data. Often, CBP cruises spanned multiple days, so modeled hypoxic volumes were averaged over the same duration as the CBP cruises. Model skill [*Wilmott*, 1981] for 2003–2004 hypoxic volume is 0.91.

4.2. River Discharge

[19] To evaluate the influence of the seasonal variation in buoyancy inputs, the model was run setting the river discharge for all tributaries equal to the annual mean value for 2004 (*Qconst*), with all other forcing consistent with the base model run. As shown in Figure 5a, the seasonal cycle of hypoxic volume is not altered in a significant way from the base model run suggesting that the temporal variability of river discharge is not the dominant factor controlling the seasonal cycle of hypoxia. Next, the overall magnitude of river discharge was varied systematically to encompass an order of magnitude change in forcing. Specifically, the discharge values for all tributaries was reduced to 20% (*Q0.2*), reduced to 50% (*Q0.5*) and doubled (*Q2*) from the observed 2004 values. These changes to river discharge exceed the range of annual averages recorded over the 43 years of data at the USGS gauging station at Conowingo. It should be noted that 2004 had the third highest annual discharge recorded at Conowingo, behind only 1972 and 2011. Doubling the river discharge for this year would have exceeded the

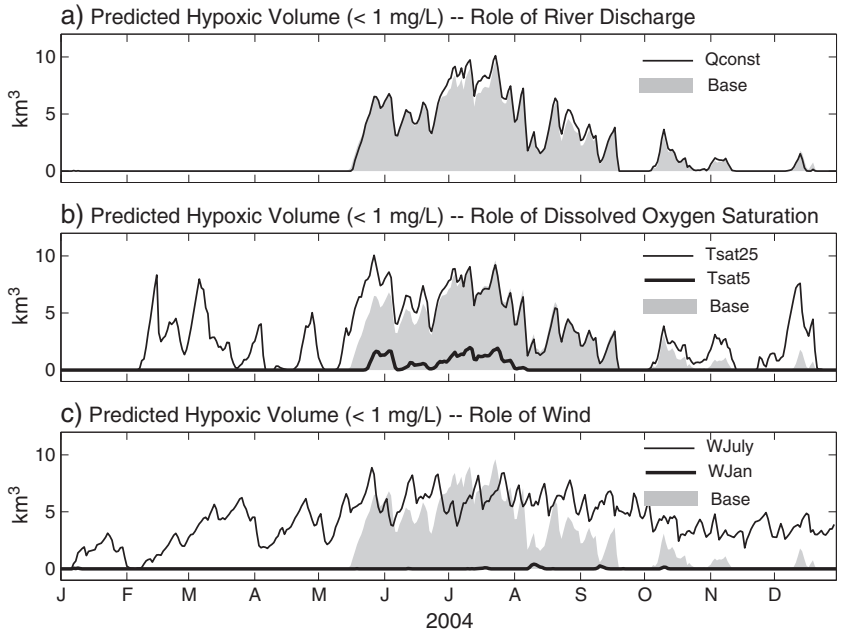

Figure 5. Comparison of the predicted hypoxic volume (<1 mg/L) for the base model run (shaded gray area) with models runs where (a) river discharge was held constant (thin black line); (b) dissolved oxygen saturation was calculated assuming a constant temperature of 25°C (thin black line) or 5°C (thick black line); (c) winds from July were repeated throughout the year (thin black line), or winds from January were repeated throughout the year (thick black line).

highest annual discharge ever recorded. Similarly, reducing the 2004 annual discharge by 20 results in an annual average smaller than any year recorded. For comparison, there are 24 years with annual discharges smaller than the *Q0.5* simulation.

[20] These large changes in river discharge had significant consequences for the total predicted hypoxic volume (Table 2). Reducing the discharge to 20% of the base reduced the total integrated hypoxic value by 50 to nearly 75%, depending on which threshold value for hypoxia was used. A reduction in discharge by 50% reduced the integrated hypoxic volume by roughly 30%. Doubling the river discharge had a smaller impact, resulting in slightly increased hypoxic volumes. In general, the greatest proportional changes in response to river discharge were observed for the anoxic with the smallest proportional changes for the mildly hypoxic volume.

4.3. Water Temperature

[21] Changes in water temperature can play a role in modulating rates of biologic processes. However, from a physical point of view, water temperature also controls the solubility of dissolved oxygen in water. Simply put, warm water can hold less dissolved oxygen at saturation than colder water. The effect of temperature on solubility in this model impacts dissolved oxygen in two ways: (1) through the initial concentration in January and (2) through the surface flux, which is proportional to saturation difference (i.e., equation (1)). To evaluate the role that seasonal changes in dissolved oxygen saturation have on hypoxia, two runs were conducted: *Tsat5* and *Tsat25*. For *Tsat5*, the model was initialized on 1 January 2004 with values of dissolved oxygen based on the saturation at 5°C, and the surface flux was calculated assuming the surface waters had a dissolved oxygen saturation based on a temperature of 5°C. Since the model does not preclude supersaturation, this has the effect of increasing the amount of dissolved oxygen that can be carried in the water by increasing the saturation. It also removes the seasonal dependence of dissolved oxygen saturation on seasonal changes in temperature. Similarly, the model run *Tsat25* was initialized on 1 January 2004 with values of dissolved oxygen based on the saturation of water at 25°C, and the surface flux was calculated assuming the surface waters had a dissolved oxygen saturation based on a temperature of 25°C. Removing the seasonal

Table 2. Integrated Hypoxic Volumes Predicted by Model[a]

Model Run	Integrated Hypoxic Volume (km^3days)		
	<0.2 mg/L	<1 mg/L	<2 mg/L
Base model run			
B	208.4	641.1	1274.3
River discharge runs			
Qconst	236.0	680.4	1312.5
Q0.2	54.8	259.5	639.1
Q0.5	135.1	464.3	996.1
Q2	233.6	686.7	1313.7
Temperature runs			
Tsat5	1.8	66.4	203.1
Tsat25	318.3	1043.2	2075.2
T+1	240.5	722.9	1399.8
T−1	184.5	582.8	1167.0
Wind runs			
W-Jan	0	3.3	126.1
W-July	517.5	1551.0	2664.6
W+0.10	69.2	347.6	864.1
W−0.10	421.5	978.1	1702.2
W+180°	70.5	335.7	853.8
W+90°	258.5	677.0	1267.3
W−90°	251.2	675.8	1274.2

[a]For each model run, the total volume of water with dissolved oxygen concentration below 0.2, 1, and 2 mg/L was calculated at each time step and integrated in time.

variation in dissolved oxygen saturation had a pronounced impact on the seasonal cycle of hypoxia (Figure 5b). For *Tsat25*, dissolved oxygen concentrations are reduced below 1 mg/L in early February, and hypoxic water is observed in every subsequent month for the rest of the year. In contrast, when dissolved oxygen saturation is based on a temperature of 5°C, the integrated hypoxic volume is reduced by nearly an order of magnitude (Table 2), with minor hypoxic conditions occurring in June and July.

[22] Given the strong seasonal changes in water temperature observed in the bay, assuming that dissolved oxygen saturation remains constant throughout the year is not realistic. In order to more realistically simulate the observed interannual variability in water temperature, air temperature values were increased ($T+1$) or decreased ($T-1$) by one standard deviation based on the 1986–2011 monthly averaged climatology observed at TPL. Altering the air temperature in the model forcing changes the sensible heat flux providing a relatively simple method for simulating interannual variations in water temperature. The observed air temperature at TPL in 2004 was slightly above average, and increasing the temperature each month by the observed standard deviation resulted in the second warmest year on record. Reducing the air temperature each month by one standard deviation resulted in the coldest year on record; thus, these runs basically span the interannual variation in air temperature observed over 25 years at TPL. The resulting water temperature, when averaged over the entire year and over the entire main stem of the bay, was increased/decreased by roughly 1°C for $T+1/T-1$. This range in water temperature is consistent with the maximum and minimum observed annual mean water temperature at TPL. Even these relatively modest changes in water temperature had a noticeable change in integrated hypoxic volume, with the warmer run having roughly 25% greater integrated hypoxic volume as compared to the colder run. Again, similar to the response to river discharge forcing, the relative changes to the anoxic volume were greater than for either definition of hypoxic volume.

4.4. Wind Speed and Direction

[23] As demonstrated in Figures 2d–2f, there is a pronounced seasonal variability in both wind speed and wind direction over Chesapeake Bay. To evaluate the role of seasonal changes in wind forcing, the model was run where the January (*W-Jan*) and July (*W-July*) wind forcing was repeated each month of the year. By forcing the model in this manner, the winds have daily variations associated with the passage of weather systems, but the seasonal changes in speed and direction are removed. The seasonal cycle of predicted hypoxic volume is strongly influenced by the seasonal cycle of wind forcing. For the case where the wind conditions in January are repeated all year, essentially no anoxic or strongly hypoxic water is predicted (Figure 5c). In contrast, when the winds from July are repeated for a complete year, the hypoxia is extensive. Hypoxic conditions begin in January and persist throughout the rest of the year. There is still a seasonal cycle, with more extensive hypoxia in summer and early fall than in the winter months, presumably because of the dependence on water temperature.

[24] Although illustrative, these simulations do not represent realistic variations in wind forcing. Further, the changes are complicated by differences in both wind speed and wind direction. Additional runs were conducted to systematically evaluate the importance of variations in wind speed and direction separately. Variations in wind speed were examined by increasing ($W+0.10$) and reducing ($W-0.10$) the summer (May–August) wind magnitude by 10% (roughly one standard deviation based on the Thomas Point Light climatology). Changes in summer wind speed had large impacts on the predicted integrated hypoxic volume. When summer wind speeds were increased, the integrated hypoxic volume was reduced by roughly 50%. Similarly, decreases in summer wind speed resulted in large increases in hypoxic and anoxic volumes (Table 2). It is worth pointing out that the observed winds over water at TPL are significantly stronger than the regional NARR model winds (i.e., Figure 2f). Forcing the model with the NARR winds resulted in over a threefold increase in hypoxic volume, presumably because of the large difference in magnitude (data not shown).

[25] Previous work has suggested that hypoxic volume in the bay is also sensitive to wind direction [*Scully* 2010a; *Scully* 2010b]. In order to try and evaluate the importance of wind direction, summer wind direction was also systematically varied in the model forcing. As is typical in most summers, the winds during the 2004 summer were predominately from the south. Sensitivity runs were conducted where the modeled wind forcing during the summer months (May–August) was rotated by positive 90° ($W+90°$), negative 90° ($W-90°$), and 180° ($W180°$), resulting in model forcing that had mean summer winds from the west, east, and north, respectively. As with changes in wind speed, there were appreciable changes in the integrated hypoxic volume related to wind direction. The least amount of hypoxic volume was predicted when the summer wind direction was from the north ($W180°$). The reduction in hypoxic volume due to simply rotating the winds 180° was comparable to a 10% increase in summer wind speed (Table 2). The integrated anoxic and strongly hypoxic volumes were greatest when mean summer wind came from the west ($W+90°$), but the base model run (*Base*) had the greatest mildly hypoxic volume. Winds from the east ($W-90°$) generally increased hypoxic volumes.

5. Discussion

5.1. River Discharge

[26] One of the surprising results presented above was the lack of sensitivity of the modeled hypoxic volume to temporal changes in river discharge (Figure 5a). The onset of stratification and the drawdown of dissolved oxygen in early summer is typically linked to elevated spring river discharge. Figure 6a shows the time series of daily Susquehanna River discharge for 2004. While discharge is generally elevated in the early spring, there is considerable variability throughout the year. In fact, most years have discharge that does not vary smoothly as depicted in Figure 2a but has significant synoptic variability associated with storm events. The highest discharge in 2004 was in mid-September associated with the remnants of Hurricane Ivan moving over the region. In 2004, the average Susquehanna River discharge for January–May was roughly the same as the annual average. As a result, when averaged over the entire summer period, the mean stratification for the base run and the run with constant river discharge (*Qconst*) are similar (Table 3).

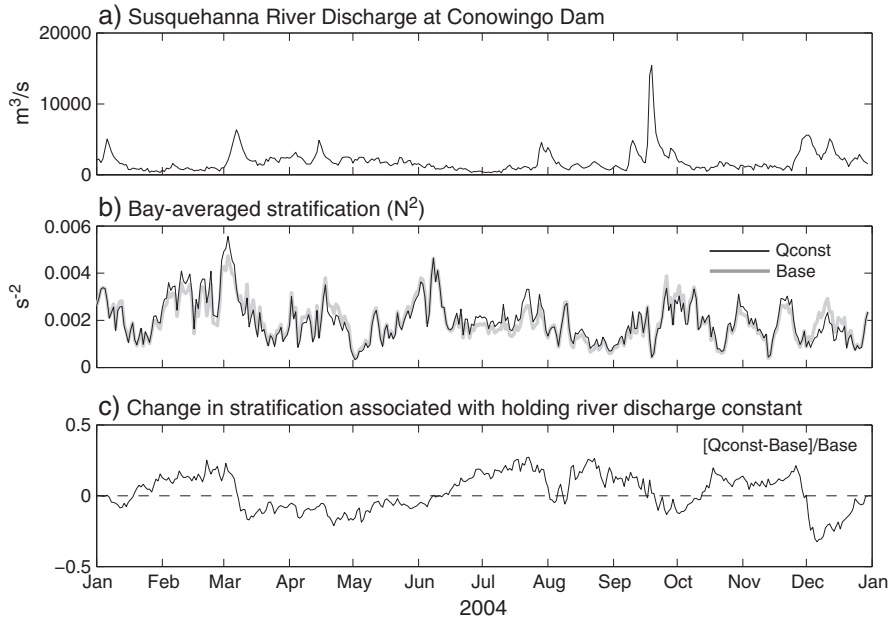

Figure 6. (a) Susquehanna River discharge for 2004 from USGS gauging station at Conowingo, MD; (b) averaged stratification over the main stem of Chesapeake Bay (shaded area in Figure 1) for the model run where river discharge was held constant (thin black line) and for the base model run with variable river discharge (thick gray line); (c) relative change in stratification associated with holding river discharge constant calculated as the difference between *Qconst* and *Base*, normalized by *Base*. Positive values indicate higher stratification for *Qconst* than *Base*.

Table 3. Averaged Pycnocline Values of N^2 and Vertical Turbulent Oxygen Flux Through the Pycnocline for All Model Runs[a]

	Average Summer Pycnocline N^2 (s^{-2})			Average Summer Pycnocline Oxygen Flux (g O_2/m^2/day)		
Model Run	Upper	Lower	All	Upper	Lower	All
Base model run						
B	4.8×10^{-3}	5.4×10^{-3}	5.2×10^{-3}	1.38	1.30	1.33
River discharge runs						
Qconst	5.3×10^{-3}	5.5×10^{-3}	5.4×10^{-3}	1.31	1.27	1.28
Q0.2	2.2×10^{-3}	2.1×10^{-3}	2.1×10^{-3}	1.74	1.76	1.75
Q0.5	3.9×10^{-3}	3.5×10^{-3}	3.6×10^{-3}	1.50	1.50	1.50
Q2	4.4×10^{-3}	7.7×10^{-3}	6.6×10^{-3}	1.39	1.13	1.21
Temperature runs						
Tsat5	4.8×10^{-3}	5.4×10^{-3}	5.2×10^{-3}	1.69	1.46	1.54
Tsat25	4.8×10^{-3}	5.4×10^{-3}	5.2×10^{-3}	1.40	1.35	1.36
T + 1	4.9×10^{-3}	5.5×10^{-3}	5.3×10^{-3}	1.38	1.29	1.32
T − 1	4.7×10^{-3}	5.3×10^{-3}	5.1×10^{-3}	1.39	1.31	1.33
Wind runs						
W-Jan	5.3×10^{-3}	3.9×10^{-3}	4.4×10^{-3}	1.73	1.38	1.49
W-July	5.1×10^{-3}	6.5×10^{-3}	6.0×10^{-3}	1.42	1.18	1.26
W + 0.10	4.0×10^{-3}	4.7×10^{-3}	4.5×10^{-3}	1.44	1.36	1.39
W − 0.10	5.6×10^{-3}	6.0×10^{-3}	5.9×10^{-3}	1.31	1.23	1.25
W + 180°	5.7×10^{-3}	4.9×10^{-3}	5.1×10^{-3}	1.67	1.45	1.52
W + 90°	6.7×10^{-3}	5.8×10^{-3}	6.1×10^{-3}	1.51	1.27	1.35
W − 90°	5.3×10^{-3}	5.3×10^{-3}	5.3×10^{-3}	1.42	1.37	1.38

[a] The pycnocline is defined as the vertical position where the maximum value of N^2 is observed at any given time step. Values were first averaged over the entire summer (May–August) and then spatially averaged over the main stem region of the bay shown in Figure 1. Averages over the upper and lower bay regions shown in Figure 1 are also reported.

[27] This is not to imply that temporal variations in river discharge are not important to temporal variations in stratification. Figure 6b plots the stratification for the base model run and *Qconst* as a function of time. Also plotted is the deviation in stratification for the *Qconst* run, normalized by the base model stratification ([*Qconst* − *Base*]/*Base*). There

are clear temporal deviations in stratification that result from holding the river discharge constant. After significant discharge events, the stratification for *Qconst* is reduced relative to the base model run, which responds to the variable buoyancy input. In fact, the deviation in stratification has a strong negative correlation ($r = -0.78$) with Susquehanna River discharge when lagged by 8 days. This response time of 8 days is much more rapid than the response time implied in Figures 2b and 2c. The response time implied by lagged correlation analysis is shorter in the upper bay (~5 days) and somewhat longer in the lower bay (~13 days). This suggests that the stratification responds relatively rapidly to changes in river discharge, which has significant variability at the event scale.

[28] While these results suggest that the seasonal cycle of hypoxia is relatively insensitive to the synoptic (5–14 days) variability of river discharge, significant changes in hypoxic volume were predicted when the overall magnitude of river discharge was varied at longer time scales. In the simulations presented above, the annual river discharge was varied by an order of magnitude. These large changes in buoyancy forcing were accompanied by significant changes in stratification (Table 3). Estuarine theory suggests that the stratification should increase with river discharge following a 2/3 power law [e.g., *Geyer* 2010]. The model runs presented here show a somewhat weaker dependence, with a roughly 1/2 power law dependence for values averaged over the entire main stem. While stratification over the majority of the main stem of the bay goes up with increasing river discharge, in the uppermost reaches of the bay the stratification goes down with increased discharge (Figure 7). In this region, the increased river discharge displaces the salt intrusion seaward, and the resulting decreases in stratification are the result of advective processes.

[29] As expected, increases in stratification associated with increased river discharge generally resulted in weaker vertical oxygen flux through the pycnocline (Table 3; Figure 8). However, it is worth pointing out that the order of magnitude variation in river discharge changed the vertical flux of oxygen through the pycnocline by less than a factor of 2. Further, there is considerable spatial variability in where the vertical flux occurs (Figure 8). For the lowest river discharge run (*Q0.2*), the greatest increases in vertical oxygen flux are over the shallower shoals regions on either side of the deep channel. The differences in vertical flux through the pycnocline over the deeper channel areas (>15 m) are considerably smaller. Similarly, the decrease in vertical mixing associated with the highest river discharge run (*Q2*) was mainly over shallower regions. Thus, the regions where there is the greatest difference in vertical flux due to changes in river discharge are the shallower regions where hypoxia is less common.

[30] The results above suggest that stratification responds to both short-term variations in river discharge (5–14 days) as well as at much longer time scales (>100 days). These two time scales can be thought of in the theoretical framework proposed by *MacCready* [2007], in which the response of an estuary to changes in forcing are represented as perturbations from the mean state. This theory predicts the time scale of the unsteady response (short-term), but there is also a steady response to the slowly varying mean forcing (long-term). In simulations covering a much longer time period, *Xu et al.* [2012] found that the stratification in Chesapeake Bay was significantly correlated to a 240 day running average of river discharge, when lagged by 64 days. A 240 day running average significantly damps the synoptic variations in river discharge, highlighting the overall response to seasonal to interannual variations in discharge. Clearly, by focusing our attention on only 1 year, this study does not resolve the role of low frequency changes in discharge. However, the overall increase in stratification and hypoxic volume associated with increases in the overall magnitude of river discharge is consistent with this longer-term response.

[31] The similarity in the seasonal cycle of hypoxia predicted by the base run and *Qconst* suggests that the time scale for the response of stratification to river discharge (~weeks) is much shorter than the time scale for oxygen drawdown (~months). As a result, the hypoxic volume does not respond strongly to variations in stratification at synoptic time scales. In contrast, variations in stratification at time scales that are long compared to the time scale for oxygen drawdown are expected to have a more significant impact on hypoxic volume. River discharge from the Susquehanna exhibits large synoptic variability (e.g., Figure 6a), and only when averaged over several years does the clear seasonal cycle emerge (e.g., Figure 2a). So, while the seasonal cycle of river discharge may play some role in the seasonal cycle of hypoxia, the results above suggest that seasonal variations in wind speed are much more important. The overall magnitude of river discharge does vary considerably from year to year, and the results presented above suggest that hypoxic volumes will respond to changes in river discharge at these longer time scales.

[32] Changes in river discharge also play a significant role in controlling the along-estuary advective flux of dissolved oxygen. Figure 9 shows the residual along-channel circulation predicted by the model near the southern limit of the hypoxic region (~ 37.5°N). As predicted by estuarine theory, there is a consistent increase in the exchange flow with increasing river discharge. In fact, dependence on river discharge predicted by the model at this location is similar to the theoretical power law dependence of 1/3. The increased residual flow with increased discharge also impacts the oxygen dynamics by advecting oxygen into the lower portion of the hypoxic region. Estimates of oxygen flux associated with the residual velocity shown in Figure 9 generally increase with increasing river discharge (Table 4). The order of magnitude increase in river discharge from *Q0.2* to *Q2*, results in nearly a 70% increase in the longitudinal advective oxygen flux at this location.

[33] As seen in Figure 10, decreased river discharge generally increases bottom dissolved oxygen concentrations throughout the main stem regions of the bay. This is generally consistent with the overall patterns of increased turbulent flux of oxygen through the pycnocline (Figure 8). However, near the mouth, bottom oxygen concentration goes down with decreased river discharge even though the turbulent flux of oxygen increases with river discharge in this area. This is because the reduced river discharge results in a reduction in the longitudinal advective flux. Doubling the river discharge only decreases the bottom dissolved oxygen concentration over the middle portion of the main stem of the bay (~37.5°N–38.5°N). The increased along-channel advective flux of dissolved oxygen associated with doubling the river discharge effectively prevents the hypoxic region from spreading further down the bay, even though the turbulent flux of oxygen through the pycnocline is substantially reduced in the lower bay associated

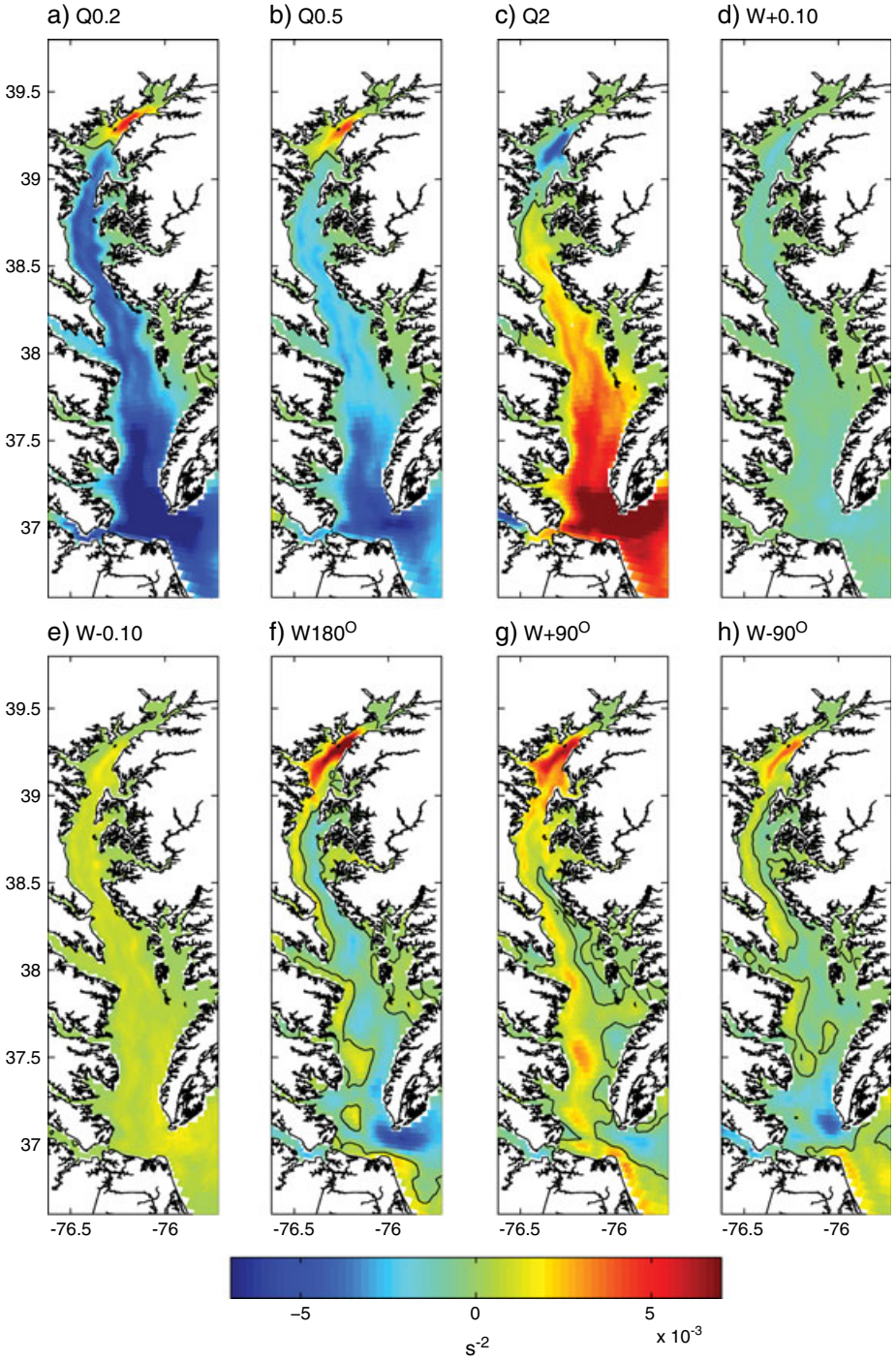

Figure 7. The deviation in summer stratification from the Base model run (model minus *Base*). Stratification is quantified as the pycnocline value of N^2 and averaged for the period May–August. Positive values indicate that the predicted stratification is greater than the Base model run. Thin black line is the zero contour.

with the increased stratification. Increases in river discharge also push the limit of salt intrusion seaward, shifting the northern limit of hypoxic water to the south. As a result, the sensitivity of hypoxic volume to river discharge is moderated because of the competing influence of increases in stratification (decreasing mixing), increased advective flux through the seaward boundary, and the decrease in overall length of the estuary.

5.2. Water Temperature

[34] Unlike the other variables considered here, temperature does not contribute to the overall estuarine dynamics at leading order. Temperature only has a minor influence on vertical density stratification in the bay. The model run with increased latent heat flux ($T + 1$) demonstrated increases in temperature for both surface and bottom waters, having little impact on the vertical thermal gradient except near the mouth.

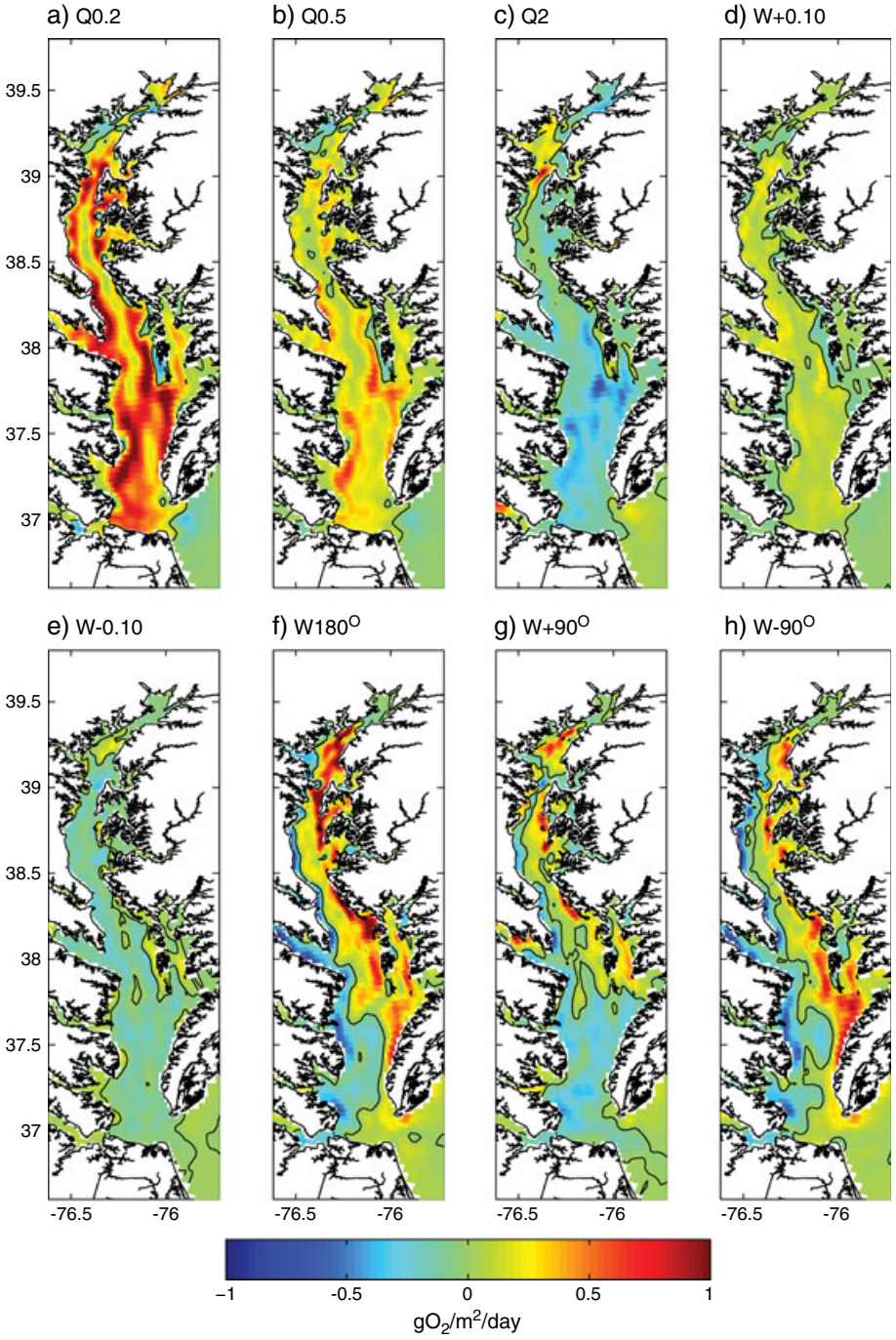

Figure 8. The deviation from the Base model run of the summer vertical turbulent oxygen flux through the pycnocline (model minus *Base*). Values are averaged for the period May–August. Positive values indicate that the predicted flux is greater than in the Base model run. Thin black line is the zero contour.

Increased air temperatures in summer slightly decreased the surface momentum flux by increasing atmospheric stability, altering the bulk momentum flux formulation. The very slight changes in stratification (<4%) reported in Table 3 are more likely due to wind stress effects than actual thermal gradients. Yet despite the small influence that temperature has on stratification, realistic changes in temperature forcing had significant impact on the oxygen dynamics. Predicted hypoxic volumes were roughly 25% bigger in $T + 1$ as compared to $T - 1$. This 25% change in hypoxic volume was associated with a roughly 2°C increase in bay-wide temperature. *Najjar et al.*, 2010 documented a roughly 1°C increase in bay water temperatures from the 1960s to the 1990s and suggested that bay-wide water temperatures will increase anywhere from 2 to 6°C by the end of the 21st century. These simulations suggest that temperature increases of this magnitude could have a significant impact on overall levels of hypoxia in the bay.

[35] Model runs *Tsat5* and *Tsat25* had the exact same hydrodynamic forcing as the base model run, so stratification values were identical. Yet, the difference in the total

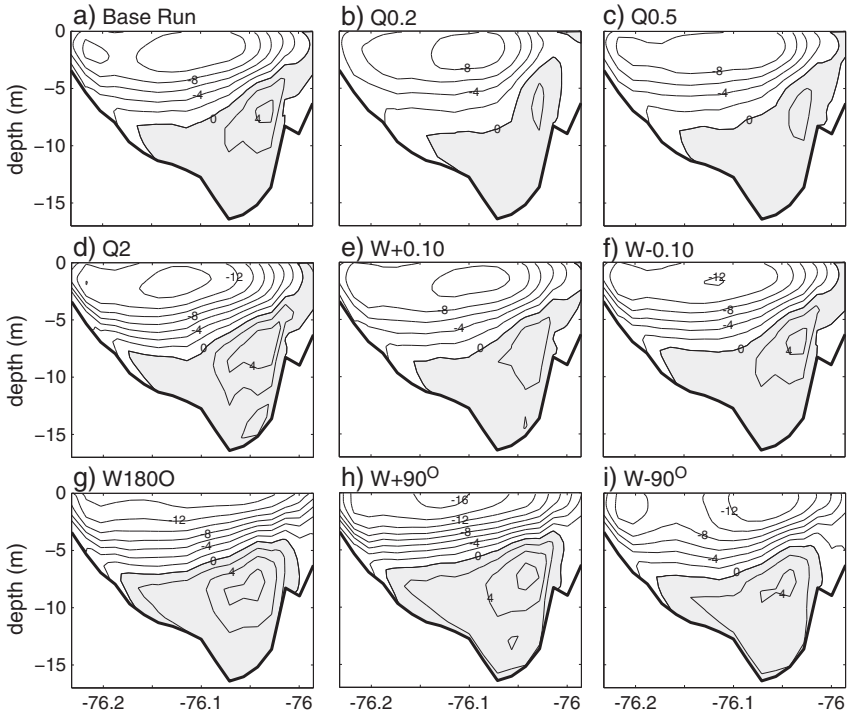

Figure 9. The tidally averaged along-channel residual circulation averaged over May–August at the southern end of the hypoxic region (37.5°N). Contour interval is 2 cm/s with positive values (shaded gray) indicating flow into the estuary. Advective oxygen flux values reported in Table 4 were calculated by averaging over the inflowing shaded regions shown above.

Table 4. Tidally Averaged Estuarine Exchange Flow and the Associated Advective Oxygen Flux Predicted by the Model at the Southern Limit of the Hypoxic Zone (37.5°N)[a]

Model Run	Estuarine Exchange Flow at 37.5°N (m/s)	Up-Estuary Advective Oxygen Flux at 37.5°N (g O_2/m^2/day)
Base model run		
B	0.085	0.984×10^4
River discharge runs		
Qconst	0.084	0.887×10^4
Q0.2	0.058	0.701×10^4
Q0.5	0.069	0.830×10^4
Q2	0.110	1.233×10^4
Temperature runs		
Tsat5	0.085	1.714×10^4
Tsat25	0.085	0.905×10^4
T + 1	0.085	0.987×10^4
T − 1	0.084	0.983×10^4
Wind runs		
W-Jan	0.145	2.725×10^4
W-July	0.084	0.905×10^4
W + 0.10	0.079	0.982×10^4
W − 0.10	0.091	0.984×10^4
W + 180°	0.118	1.822×10^4
W + 90°	0.120	1.525×10^4
W − 90°	0.092	1.192×10^4

[a]Values were averaged in time over the entire summer (May–August). The estuarine exchange flow was calculated as the difference between the cross-sectionally averaged velocity of the inflowing water (positive) minus the cross-sectionally averaged outgoing water (negative). The advective oxygen flux was calculated as the product of the along-channel velocity and the dissolved oxygen concentration, averaged over the part of the cross-section where the residual velocity was directed landward.

vertical flux through the pycnocline for these two runs is quite different (Table 3). On average, the surface concentration of dissolved oxygen was roughly 50% greater in *Tsat5* than *Tsat25*. As a result, even with the same stratification and eddy diffusivity, *Tsat5* had significantly higher turbulent fluxes through the pycnocline. In addition to highlighting the role that temperature plays in controlling oxygen saturation, this result also points out the importance of understanding the surface oxygen flux. In this model, we employ a wind speed dependent piston velocity. Results were not significantly different in model runs where the piston velocity was constant or in runs where surface oxygen concentration was simply set to the saturation value. Perhaps more importantly, this result also demonstrates a significant shortcoming of this model—the lack of biologic oxygen production. Observation of surface dissolved oxygen concentrations in Chesapeake Bay often are supersaturated during summer months. This supersaturation is the result of in situ oxygen production by phytoplankton. The fact that *Tsat5* has roughly 10% greater vertical oxygen flux than *Tsat25* suggests that the dissolved oxygen concentration in surface waters impacts the magnitude of vertical flux through the pycnocline. As a result, in situ oxygen production in surface waters may be important to the magnitude and spatial distribution of vertical flux through the pycnocline.

5.3. Wind Speed and Direction

[36] Simulations of hypoxic volume show significant variability in response to both wind speed and direction. As expected, increased/decreased summer wind speeds (*W + 0.10* and *W − 0.10*) result in decreased/increased

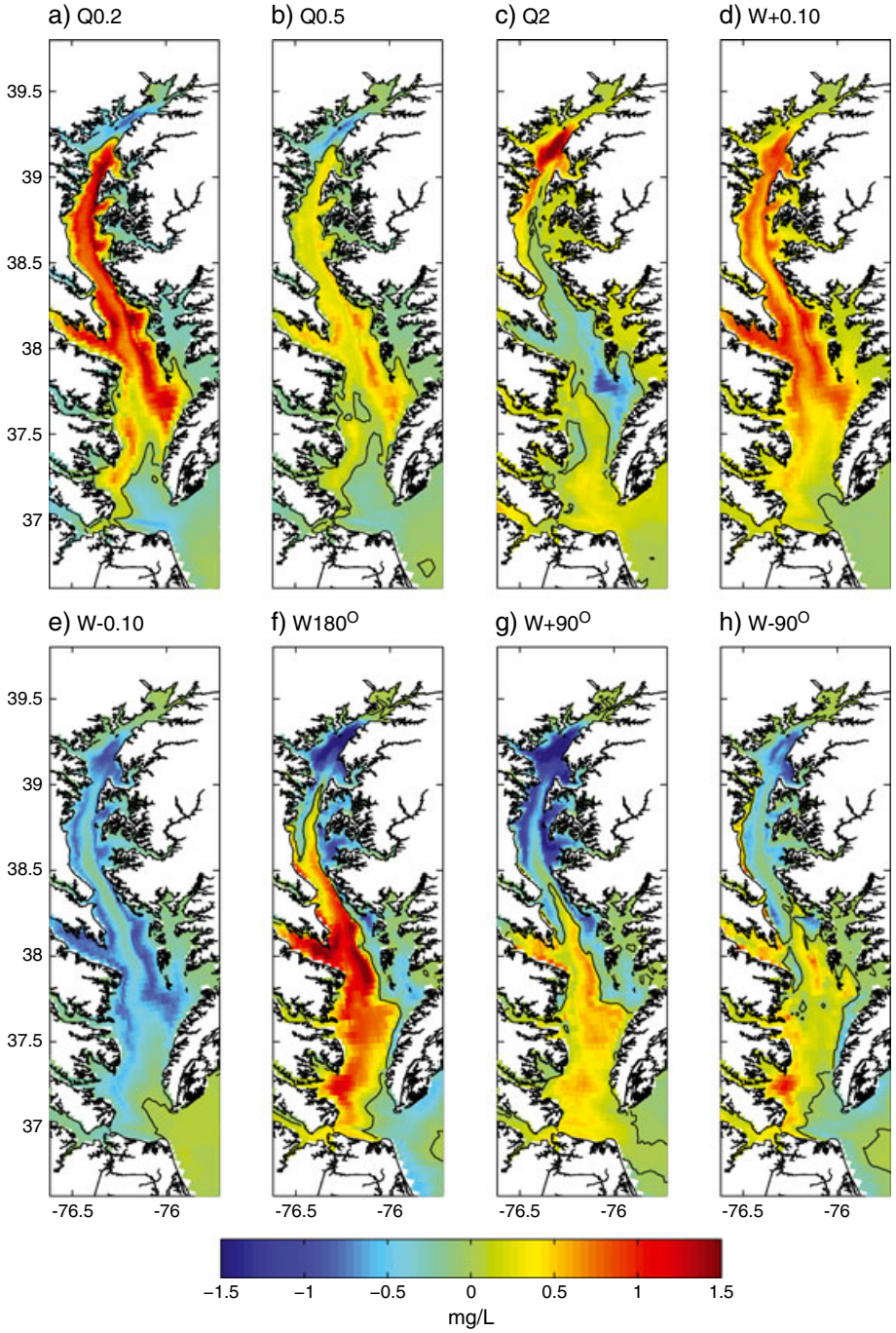

Figure 10. The deviation from the Base model run of the bottom dissolved oxygen concentration (model minus *Base*). Values are averaged for the period May–August. Positive values indicate that the predicted bottom dissolved oxygen concentration is higher than the Base model run. Thin black line denotes the zero contour.

overall levels of stratification (Figure 7, Table 3), with $W + 0.10$ having roughly 30% lower stratification than $W - 0.10$, on average. The increased stratification associated with decreased wind speed resulted in a roughly 10% decrease in vertical flux of dissolved oxygen through the pycncoline. Increased/decreased wind speeds generally increase/decrease bottom dissolved oxygen concentrations throughout the bay, with the greatest changes observed in the intermediate depth regions immediately flanking the deep channel (Figure 10).

[37] Changes in wind direction also significantly impact stratification and vertical oxygen flux. As seen in Figure 7, the impact of wind direction on stratification has considerable spatial variability. When the mean summer wind direction is from the north (*W180°*), stratification is enhanced in the upper reaches of the bay. In this region, the bay is relatively narrow, and it appears that the axial straining mechanism proposed by *Scully et al.* [2005] dominates. In the middle reaches, where the bay is wider, values of stratification are roughly the same for *Base* and *W180°*. However, because of the rotational

response to wind forcing, stratification is enhanced on the western side of the bay in response to winds from the north and enhanced on the eastern shore in response to winds from the south. This is not simply the result of pure lateral straining [*Li and Li*, 2011], which would increase stratification everywhere in response to up-estuary winds, but of the interaction between lateral straining and turbulent mixing. On average, the lower regions of the bay exhibit greater stratification when winds blow from the south (*Base)* than from the north (*W180°*).

[38] Increased stratification in the lower bay in response to winds from the south could be attributed to lateral straining as discussed in *Li and Li* [2011]. However, the observed changes in stratification in the lower bay are complicated by the change in orientation at the bay mouth. Unlike the majority of the bay, where the channel runs north-south, the axis at the mouth runs east-west. *Valle-Levinson et al.* [2001] demonstrated that the Ekman response to winds from the south enhances the two-layer exchange at the mouth, increasing stratification in the lower bay. In contrast, winds from the north surface reduce the baroclinic exchange at the mouth favoring reduced stratification. The lower bay is further complicated by the significant inputs of buoyancy from the Potomac, Rappahannock, York, and James Rivers, whose combined discharge is roughly half of the Susquehanna's annual input. The significant source of buoyancy entering the lower bay along the western shore further complicates the rotational response to along-channel wind forcing.

[39] In general, the spatial patterns of vertical oxygen flux are qualitatively similar to the spatial patterns in stratification (Figure 8). Yet, there are significant quantitative differences in response to along-channel wind forcing. Despite roughly equal average stratification, the run with mean winds from the North (*W180°*) has significantly larger vertical oxygen flux than the base case. This is particularly evident in the upper reaches of the bay where stratification is significantly enhanced in *W180°* relative to *Base* yet shows higher turbulent oxygen flux. The strong axial straining in response to down-estuary winds has two additional effects: (1) enhanced up-estuary near-bed flow (which increases bed stress) and (2) increased vertical shear across the pycnocline. Both of these two processes act to increase the vertical eddy diffusivity and enhance mixing. Thus, while down-estuary winds may increase stratification in the upper bay, the model also predicts enhanced vertical oxygen flux in this region. While the deviation in stratification associated with *W180°* changes sign from the upper to lower bay, the stratification increases bay-wide when the mean summer wind direction is rotated to blow from the west ($W+90°$). In fact, $W+90°$ demonstrates the greatest stratification of any wind direction considered. Compared to the base model run, stratification is enhanced over nearly the entire main stem domain (Figure 7). $W-90°$ demonstrates increased stratification over large portions of the upper and middle bay but overall lower stratification near the mouth. Even though both $W+90°$ and $W-90°$ have greater average stratification than the base run, they also both have greater average vertical oxygen flux across the pycnocline.

[40] In the upper portion of the bay, the vertical flux of oxygen is larger than the base model run for all three wind directions considered. Yet, the upper bay region generally has higher oxygen concentrations in the base model run than *W180°*, $W+90°$, or $W-90°$, suggesting that advective processes play an important role in controlling the distribution of hypoxia. The increase in hypoxic conditions in the lower bay for the base model run can be attributed to the weak residual circulation and along-estuary oxygen flux that accompanies winds from the south. In contrast, the model runs with mean winds from both the north (*W180°*) and the west ($W+90°$) generally have the strongest residual circulation and associated advective flux of oxygen. The strong increase in estuarine residual seen for mean winds from the west highlights the importance of rotation in the dynamics of Chesapeake Bay. Winds from the west drive down-estuary flow due to Ekman dynamics, with a compensating return flow at depth. This not only increases the residual estuarine exchange flow, but it also increases stratification via straining and brings oxygenated water into the southern end of the hypoxic zone. The impact of this advective flux of dissolved oxygen can be clearly seen in Figure 10, where bottom dissolved oxygen concentrations in the lower bay are generally increased when the mean summer winds shift to blow from the west. The weakest residual circulation and associated longitudinal oxygen flux is observed for the Base model run. Shifting winds to any other direction generally increases the horizontal advective flux through the seaward end of the hypoxic region (Table 4) and increases bottom oxygen concentrations in the lower bay relative to the Base case (Figure 10). Overall changes in wind speed have a relatively modest impact on the strength of the along-channel residual circulation (Figure 9). Because winds come primarily from the south during the summer, increases in wind speed generally reduce the residual circulation and the associated advective oxygen flux (Table 4). In contrast, weaker winds have stronger along-channel residual flow and greater advective oxygen flux.

[41] Although not realistic, the simulation where January winds were repeated throughout the year (*W-Jan*) provides further insight into the importance of along-channel advection to the seasonal cycle of hypoxia. The averaged summer estuarine velocity was highest for this run, and the advective oxygen flux at the traditional southern limit of the hypoxic zone was nearly three times that of the base model run (Table 4). Winds over Chesapeake Bay during the winter months are predominantly from the north. These strong, down-estuary winds result in strong estuarine residual velocities that both create stratification and provide oxygen to the lower portion of the bay. As a result, even though *W-Jan* had significantly stronger average stratification than *Q0.2* and *Q0.5*, *W-Jan* did not develop any anoxic water during the summer months. In comparison, *Q0.2* and *Q0.5* had appreciable hypoxia throughout the summer, despite the fact that the average turbulent flux of oxygen through the pycnocline was greater for these runs. A significant reason why no hypoxia is predicted in *W-Jan* is the large increase in the longitudinal advective flux associated with strong winds from the north. This result suggests that seasonal changes in both wind speed and direction play a key role in the seasonal cycle of hypoxia. Not only do the strong winter winds ventilate bottom water via direct turbulent mixing, but they also drive strong residual velocities, providing an advective source of oxygen to the lower bay.

Strong winds from the south are not as effective because they reduce the strength of the estuarine residual circulation and the associated horizontal flux of oxygen.

[42] Previous modeling studies have demonstrated the importance of wind direction on the lateral advective flux of dissolved oxygen [*Scully*, 2010b]. The results of this study are largely consistent with this previous work. The predicted anoxic volume for the model run with mean summer winds from the west ($W+90°$) is roughly 25% greater than the base model run. This difference can be attributed to the lateral advective flux since both the direct turbulent flux through the pycnocline and the longitudinal advective flux are greater for $W+90$ than the base case. As discussed in *Scully* [2010b], upwelling driven by the Ekman response to along-channel wind forcing brings water with lower dissolved oxygen concentration to the surface. This enhances the atmospheric flux of oxygen into the water column via the gradient formulations in equation (1). The mixing is further enhanced down into the water column where upwelling lifts the pycnocline upward into the surface boundary layer (Figure 11). For up-estuary winds (i.e., the base model run), this upwelling occurs to the west of the channel, while down-estuary winds (i.e., $W180°$) enhance mixing east of the channel. Across-estuary winds generally have weaker lateral Ekman response, and as a result there are strong lateral asymmetries in where the vertical oxygen flux occurs as a function of wind direction (Figure 11).

5.4. Consistency with Observations of Hypoxia

[43] Both *Scully* [2010a] and *Murphy et al.* [2011] noted that interannual variations in hypoxic volume were negatively correlated with the duration of summer winds from the southeast. *Scully* [2010a] also noted a negative correlation with the duration of winds from the west but found no significant correlation between interannual variations in hypoxic volumes and mean summer wind speed. The results presented above are consistent with increased anoxic volume for winds from the west. In fact, anoxic volumes increased by roughly 25% when the mean summer winds were from the west. However, the sensitivity of hypoxic volumes was less clear. Further, the model results also show a strong dependence on wind speed that is not consistent with *Scully* [2010a]. It is important to note that the wind data used in that study were collected at the Naval Air Station (NAS) in Patuxent, MD. While this station is close to the central region of Chesapeake Bay, it is located over land and does not directly measure wind speed over water. As demonstrated in Figure 2f, there are significant asymmetries in the strength of summer winds from different directions at TPL. In an average sense, the strongest winds blow from the south, and the weakest winds blow from the west. This asymmetry between the strength of summer winds from the south and from the west is not observed at NAS (data not shown) or in the NARR model. The asymmetry in wind strength observed at TPL is consistent with spatial gradients in surface roughness associated with the adjacent land mass. A similar asymmetry is not expected in measurements made over land (particularly on the western shore). Thus, the strong dependence on wind direction reported by *Scully* [2010a] most likely includes a wind speed dependence not captured in the NAS wind.

[44] Neither *Scully* [2010a] nor *Murphy et al.* [2011] report negative correlations between hypoxic volume and the duration of summer winds from the north. In contrast, this study demonstrates significant reductions in anoxic and hypoxic volumes when the summer winds are rotated to have a mean direction from the north ($W180°$). While this model run is instructive, it is important to point out that it does not realistically simulate summer wind conditions. Mean summer winds over Chesapeake Bay are always from the south. Winds from the north do occur, associated with the passage of weather systems, but persistent down-estuary winds during summer like those used in $W180°$ are not observed. As seen in Figure 9 and Table 4, rotating the summer winds 180° significantly increases both the residual circulation and the along-channel flux of oxygen. If this increase in flux at the southern end of the hypoxic region is only temporary, the impact on the overall hypoxic volume will be modest. *Scully* [2010b] documented large reductions in hypoxic volume associated with idealized down-estuary winds. However, because the idealized wind events only lasted 3 days, the return to hypoxic conditions associated with a wind event from the north was rapid. As a result, *Scully* [2010b] found that the net impact on hypoxic volume of a single wind event from the north was smaller than a single wind event from the south. Similarly, *Li and Li* [2011] noted that stratification rebounded much more

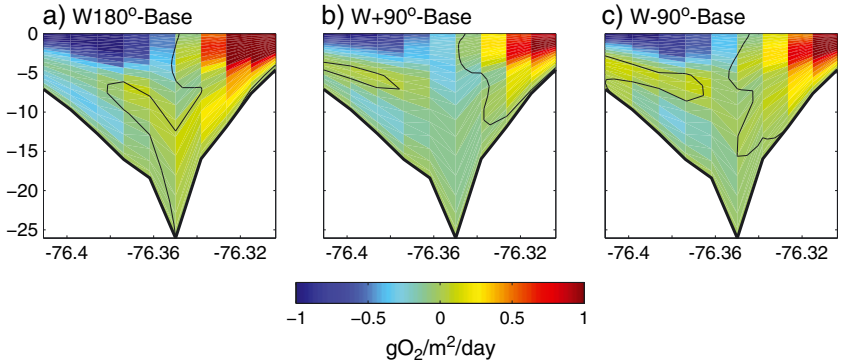

Figure 11. The deviation from the Base model run of the summer vertical turbulent oxygen flux at the estuarine cross-section located at CB4.3 for model runs (a) W180°, (b) W + 90°, and (c) W − 90°. Values are averaged for the period May–August. Positive values indicate that the predicted flux is greater than in the Base model run. Thin black line is the zero contour.

quickly after down-estuary than up-estuary wind events. However, both of these studies only considered a single idealized wind event and did not examine the importance of persistent changes in wind direction over several months, as considered here. The 180° shift in the mean summer wind direction significantly increased the along-channel oxygen flux over the entire summer. The integrated impact of this on hypoxic volume was considerably greater than the impact of a single wind event considered by *Scully* [2010b].

5.5. Limitations of the Approach

[45] It is important to point out that the approach used in this paper is a gross simplification of the biological oxygen dynamics in Chesapeake Bay. It ignores in situ oxygen production by phytoplankton, benthic oxygen demand, and the chemical oxygen demand associated with hydrogen sulfide dynamics. Given these simplifications, the prescribed oxygen utilization rate used in the model is most analogous to a net planktonic community respiration rate. There is considerable observational evidence demonstrating that the community respiration rates in Chesapeake Bay vary strongly in both time and space. *Smith and Kemp* [1995] demonstrated both seasonal and spatial variations in community respiration rates. *Smith and Kemp* [2003] reported significant along-estuary variability in community respiration rates with the highest rates observed in the central mesohaline region of the bay, with significantly smaller values in both the oligohaline and polyhaline regions.

[46] For this study, the oxygen utilization rate was simply treated as a tuning parameter, which was selected so that the predicted hypoxic volumes matched observations reasonably well. The rate used in this study falls within the bounds of values reported in the literature. For example, *Smith and Kemp* [1995] reported summer time values for Chesapeake Bay that ranged from 0.9×10^{-4} mmolO_2/m^3/s in the upper bay to 4.3×10^{-4} mmolO_2/m^3/s in the mid-bay. The constant value used in this study is generally above the values that *Smith and Kemp* [1995] reported for winter but below typical mesohaline summertime values. The predicted hypoxic volumes in this study were sensitive to the respiration rate that was used. For example, a 25% reduction in oxygen utilization rate led to roughly a factor of three reduction in spatially and temporally integrated hypoxic volume. Similarly, a 25% increase in respiration rate led to almost a doubling of hypoxic volume (data not shown). This sensitivity to the respiration rate clearly illustrates the importance of the biological dynamics that were ignored by this study. Future studies that consider interannual variations in hypoxic volume will clearly have to account for the biological variability more accurately.

6. Summary and Conclusions

[47] In this study, a three-dimensional circulation model with a relatively simple representation of oxygen dynamics was used to isolate the role of physical forcing in modulating hypoxia in Chesapeake Bay. Despite assuming that biological oxygen utilization was constant in both time and space, the model simulated the seasonal cycle of hypoxia with skill. This result highlights the important role that physical forcing plays in both the seasonal cycle of hypoxia and the interannual variability in hypoxic volumes. River discharge, water temperature, and wind forcing all had significant impacts on the overall extent of low oxygen water. Anoxic volumes (<0.2 mg/L) showed greater sensitivity to physical forcing than hypoxic volumes (<2 mg/L).

[48] The seasonal cycle of hypoxia was relatively insensitive to temporal variations in river discharge at synoptic time scales but did respond to changes in the overall magnitude of river discharge, implying sensitivity at longer time scales (longer than months). Decreases in the overall magnitude of river discharge significantly reduced simulated hypoxic volumes. This occurred largely because reduced stratification allowed for increased turbulent flux of dissolved oxygen through the pycnocline. As river discharge increased, hypoxic volumes increased, but advective processes moderated the response. Increases in river discharge both shortened the overall length of the salt intrusion and increased the influx of oxygenated water into the lower regions of the bay, effectively limiting the overall length of the hypoxic region.

[49] Simulations demonstrated that the seasonal cycle of temperature, and its control of the solubility of dissolved oxygen, contributes to the seasonal cycle of hypoxia at leading order. Simulations that assumed that the solubility of dissolved oxygen was set by water with a temperature of 5°C yearround had an order of magnitude less hypoxic volume than the base model run, where solubility followed the seasonal cycle of water temperature. An annual increase in water temperature of 2°C resulted in roughly 25% greater hypoxic volume. This increase was almost entirely due to reduced overall oxygen concentration associated with lower solubility, allowing drawdown to hypoxic conditions to occur more rapidly.

[50] Changes in wind forcing had the greatest impacts on oxygen dynamics in the model simulations considered. Wind speed and direction play a dominant role in the seasonal development of hypoxic water. During the winter months, stronger winds from the north increased both direct turbulent mixing oxygen through the pycnocline and the along-channel advective flux of oxygen into the lower bay preventing hypoxia from developing. Weaker summer winds from the south had reduced turbulent oxygen flux and lower longitudinal advective flux, allowing hypoxic conditions to develop. Persistent winds from the north are not observed during the summer months, and shifts in mean wind direction to either the east or west increased anoxic volumes relative to the simulation with mean summer winds from the south. Simulated hypoxic volumes demonstrated sensitivity to summer wind speed, with weaker winds leading to greater overall hypoxia. Direct observations of wind speed over water show that summer winds from the south are the strongest and winds from the west are weakest. This asymmetry may contribute to historical observations that show interannual variations in hypoxic volume are sensitive to subtle shifts in wind direction.

[51] **Acknowledgments.** We thank two anonymous reviewers for their thoughtful comments on this manuscript. The funding for this research was obtained from NSF Grant OCE-0954690 and supported by NOAA via the U.S. IOOS Office (Award Numbers NA10NOS0120063 and NA11NOS0120141) and managed by the Southeastern Universities Research Association.

References

Beckmann, A., and D. B. Haidvogel (1993), Numerical simulation of flow around a tall, isolated seamount. Part I: Problem formulation and model accuracy, *J. Phys. Oceanogr.*, *23*, 1736–1753.

Blumberg, A. F, and D. M. Goodrich (1990), Modeling of wind-induced destratification in Chesapeake Bay, *Estuaries*, *13*, 236–249.

Butt, A.J, and B.L. Brown (2000), The cost of nutrient reduction: A case study of Chesapeake Bay, *Coastal Management*, *28*, 175–185.

Chen, S-N, and L. P. Sanford (2009), Axial wind effects on stratification and longitudinal salt transport in an idealized estuary, *J. Phys. Oceanogr.*, *39*, 1905–1920, doi:10.1175/2009JPO4016.1.

Geyer, W. R. (2010), Estuarine salinity structure and circulation, in Contemporary Issues in Estuarine Physics, edit by A. Valle-Levinson, pp 12–26, Cambridge University Press.

Goodrich, D. M., W. C. Boicourt, P. Hamilton, and D. W. Pritchard (1987), Wind-induced destratification in Chesapeake Bay, *J. Phys. Oceanogr.*, *17*, 2232–2240.

Hagy, J. D., W. R. Boyton, C. W. Keefe, and K. V. Wood (2004), Hypoxia in Chesapeake Bay, 1950–2001: Long-term changes in relation to nutrient loading and river flow, *Estuaries*, *27*, 634–658, doi:10.1007/BF02907650.

Kantha, L. H., and C. A. Clayson (1994), An improved mixed layer model for geophysical application, *J. Geophys. Res.*, *99*, 25,235–25,266.

Kemp, W.M., et al. (2005), Eutrophication of Chesapeake Bay: Historical trends and ecological interactions, *Mar. Eco. Prog. Ser.*, *303*, 1–29, doi:10.3354/meps303001.

Large, W. G., and S. Pond (1981), Open ocean momentum flux measurements in moderate to strong winds, *J. Phys. Oceanogr.*, *11*, 324–336.

Li, M., L. Zhong, and W. C. Boicourt (2005), Turbulence mixing parameterizations and comparison with observations, *J. Geophys. Res.*, *110*, doi:10.1029/2004JC002585.

Li, Y., and M. Li (2011), Effects of winds on stratification and circulation in a partially mixed estuary, *J. Geophys. Res.*, *116*, C12012, doi:10.1029/2010JC006893.

Li, Y., and M. Li (2012), Wind-driven lateral circulation in a stratified estuary and its effects on the along-channel flow, *J. Geophys. Res.*, *117* (C9), C09005, doi:10.1029/2011JC007829.

MacCready, P. (2007), Estuarine adjustment, *J. of Phys. Oceanogr.*, *37*, 2133–2145.

Malone, T. C., W. M. Kemp, H. W. Ducklow, W. R. Boynton, J. H. Tuttle, and R. B. Jonas (1986), Lateral variation in the production and fate of phytoplankton in a partially stratified estuary, *Mar. Eco. Prog. Ser.*, *32*, 149–160.

Marino, R., and R. W. Howarth (1993), Atmospheric oxygen exchange in the Hudson River: Dome measurements and comparison with other natural waters, *Estuaries*, *16*, 433–445.

Murphy, R. R., W. M. Kemp, and W. P. Ball (2011), Long-term trends in Chesapeake Bay seasonal hypoxia, stratification and nutrient loading, *Estuaries Coasts*, *34*, 1293–1309.

Najjar, R. G., et al. (2010), Potential climate-change impacts on the Chesapeake Bay, *Estuarine Coastal Shelf Sci.*, *86*, 1–20.

Newcombe, C. L., and W. A. Horne (1938), Oxygen-poor waters of the Chesapeake Bay, *Science*, *88*, 80–81.

North, E. W., S-Y. Chao, L. P. Sanford, and R. R. Hood (2004), The influence of wind and river pulses on an estuarine turbidity maximum: Numerical studies and field observations in Chesapeake Bay, *Estuaries*, *27*, 132–146, doi:10.1007/BF02803567.

O'Donnell, J., H. G. Dam, W. F. Bohlen, W. Fitzgerald, P. S. Gay, A.E. Houk, D.C. Cohen, and M.M. Howard-Strobel (2008), Intermittent ventilation in the hypoxic zone of western Long Island Sound during the summer of 2004, *J. Geophys. Res.*, *113*, C09025, doi:10.1029/2007JC004716.

Officer, C. B, R. B. Biggs, J. L. Taft, L. E. Cronin, M. A. Tyler, and W. R. Boynton (1984), Chesapeake Bay anoxia: Origin, development, and significance, *Science*, *223*, 22–27.

Sanford, L. P., K. G. Sellner, and D. L. Breitburg (1990), Covariability of dissolved oxygen with physical processes in the summertime Chesapeake Bay, *J. Mar. Res.*, *48*, 567–590.

Scully, M. E., C. T. Friedrichs, and J. M. Brubaker, (2005), Control of estuarine stratification and mixing by wind-induced straining of the estuarine density field, *Estuaries*, *28*, 321–326, doi:10.1007/BF02693915.

Scully, M. E., (2010a), The importance of climate variability to wind-driven modulation of hypoxia in Chesapeake Bay, *J. Phys. Oceanogr.*, *40*, 1435–1440, doi:10.1175/2010JPO4321.1.

Scully, M. E., (2010b), Wind modulation of dissolved oxygen in Chesapeake Bay, *Estuaries Coasts*, *33*, 1164–1175.

Smolarkiewicz, P. K., and L. G. Margolin (1998), MPDATA: A finite-difference solver for geophysical flows, *J. Comput. Phys.*, *140*, 459–480.

Smith, E. M., and W. M. Kemp (1995), Seasonal and regional variations in plankton community production and respiration for Chesapeake Bay, *Mar. Eco. Prog. Ser.*, *116*, 217–231.

Smith, E. M., and W. M. Kemp (2003), Planktonic and bacterial respiration along an estuarine gradient: Responses to carbon and nutrient enrichment, *Aquatic Micro. Eco.*, *30*, 251–261, doi:10.3354/ame030251.

Taft, J. L., E. O. Hartwig, and R. Loftus (1980), Seasonal oxygen depletion in Chesapeake Bay, *Estuaries*, *3*, 242–247.

Valle-Levinson, A., K-C Wong, and K. T. Bosley (2001), Observations of the wind-induced exchange to Chesapeake Bay, *J. Mar. Res.*, *59*, 391–416.

Wang, D. P. (1979), Wind-driven circulation in the Chesapeake Bay, winter, 1975, *J. Phys. Oceanogr.*, *9*, 564–572.

Wilmott, C. J. (1981), On the validation of models, *Physical Geography*, *2*, 184–194.

Wilson, R. E., R. L. Swanson, and H. A. Crowley (2008), Perspectives on long-term variations in hypoxic conditions in western Long Island Sound, *J. Geophys. Res.*, *113*, doi:10.1029/2007JC004693.

Xu, J., W. Long, J. D. Wiggert, L. W. J. Lanerolle, C. W. Brown, R. Murtugudde, and R. R. Hood (2012), Climate forcing and salinity variability in Chesapeake Bay, USA, *Estuaries Coasts*, *35*, 237–261, doi:10.1007/s12237-011-9423-5.